Spatiotemporal analysis of calcium dynamics in the nucleus of hamster oocytes

Hideki Shirakawa and Shunichi Miyazaki

Department of Physiology, Tokyo Women's Medical College, Kawada-cho, Shinjuku-ku, Tokyo 162, Japan

1. Subcellular Ca^{2+} dynamics inside and around the nucleus of immature hamster oocytes were analysed with confocal Ca^{2+} imaging.
2. The ratio value between emission intensity of two injected fluorescent Ca^{2+} indicators, Calcium Green and Fura Red, was almost uniform over the entire oocyte, suggesting that nucleoplasmic Ca^{2+} concentration ($[Ca^{2+}]_n$) is comparable to cytoplasmic Ca^{2+} concentration ($[Ca^{2+}]_c$) at the resting state.
3. When Ca^{2+} was iontophoretically injected into the nucleoplasm or the perinuclear cytoplasm, it diffused across the nuclear envelope (NE), and perinuclear $[Ca^{2+}]_c$ and $[Ca^{2+}]_n$ reached the same level within 2 s, although the NE worked as a weak but detectable barrier for Ca^{2+} diffusion.
4. Inositol 1,4,5-trisphosphate (IP_3)-induced Ca^{2+} release from the NE through the inner membrane was not detected, even when a large amount of IP_3 was delivered in close proximity to the inner nuclear membrane.
5. When an oocyte was uniformly stimulated by photolysis of caged IP_3, a Ca^{2+} rise was initiated in the perinuclear cytoplasm. The $[Ca^{2+}]_n$ rise was always delayed with respect to, but rapidly equilibrated with, the $[Ca^{2+}]_c$ rise.
6. Clusters of the endoplasmic reticulum were located in the perinuclear cytoplasm and served as the trigger zone of IP_3-induced Ca^{2+} release.
7. The results indicate that the $[Ca^{2+}]_n$ rise occurs as the consequence of the influx of Ca^{2+} which was released in the perinuclear cytoplasm, not Ca^{2+} release from NE to the nucleoplasm.

Mechanisms regulating nucleoplasmic Ca^{2+} concentration ($[Ca^{2+}]_n$) are currently of major interest in the fields of cell biology, genetics and developmental biology, because nuclear Ca^{2+} is probably involved in the regulation of many events in the nucleus, such as gene expression (Roche & Prentki, 1994), DNA replication (Boynton, Whitfield & MacManus, 1980), chromatin fragmentation in apoptosis (Nicotera, Zhivotovsky & Orrenius, 1994), and breakdown and reconstruction of the nuclear envelope (NE) (Baitinger, Alderman, Poenie, Schulman & Steinhardt, 1990; Sullivan, Busa & Wilson, 1993). In germ cells, especially in oocytes, an increase in cytoplasmic Ca^{2+} concentration ($[Ca^{2+}]_c$) has long been suggested to be a key factor in the processes of cell cycle progression. The resumption of meiotic arrest of mature eggs, for example, is thought to be driven by the rise(s) in intracellular Ca^{2+} concentration at fertilization or parthenogenetic activation (Whitaker & Patel, 1990; Tombes, Simerly, Borisy & Schatten, 1992). The initiation of the maturation of immature mammalian oocytes, which are arrested at the prophase of the first meiosis, is also dependent on Ca^{2+} at least in some species (Homa, 1991; Kaufman & Homa, 1993). It is plausible that nuclear Ca^{2+} could play a regulatory role in some step(s) of these processes in oocytes, since dynamic changes in the structures of chromosomes and NEs take place during the progression of the cell cycle during maturation and fertilization.

Since the method of fluorescence ratiometry with the Ca^{2+}-sensitive dye, fura-2, was established, the temporal and spatial dynamics of intracellular Ca^{2+} have been widely investigated in a great variety of cell types. It was only a few years ago, however, that it became possible to distinguish $[Ca^{2+}]_n$ from $[Ca^{2+}]_c$, with the improvement of spatial resolution in confocal fluorescence microscopy. The comparison of changes in $[Ca^{2+}]_n$ and $[Ca^{2+}]_c$ has been made in many cell types, such as liver cells (Lin, Hajnóczky & Thomas, 1994), cardiac muscle cells (Minamikawa, Takahashi & Fujita, 1995), smooth muscle cells (Himpens, De Smedt & Casteels, 1994), lymphocytes (Furuno, Hamano & Nakanishi, 1993), mast cells (Katagiri, Takamatsu,

Minamikawa & Fujita, 1993), and neurons (Al-Mohanna, Caddy & Bolsover, 1994; O'Malley, 1994) in response to various extracellular stimuli. At present, it seems controversial whether $[Ca^{2+}]_n$ is controlled independently from $[Ca^{2+}]_c$ or not. In egg cells, changes in $[Ca^{2+}]_n$ and $[Ca^{2+}]_c$ were investigated in the Ca^{2+} responses during fertilization or maturation as well as intracellular injection of Ca^{2+}-releasing reagents, such as inositol 1,4,5-trisphosphate (IP_3), ryanodine, or cyclic ADP ribose (cADPr) (Shen & Buck, 1993; Carroll, Swann, Whittingham & Whitaker, 1994; Gillot & Whitaker, 1994; Stricker, Centonze & Melendez, 1994; Lefèvre, Pesty & Testart, 1995; Shiraishi, Okada, Shirakawa, Nakanishi, Mikoshiba & Miyazaki, 1995), but no clear evidence for the differential control of $[Ca^{2+}]_n$ has been obtained so far.

In vitro studies have suggested that the nucleus may serve as an intracellular Ca^{2+} store (see Malviya, 1994). Isolated rat liver nuclei show Ca^{2+} uptake and Ca^{2+} release from the nuclear matrix in an ATP- and IP_3-dependent manner, respectively (Nicotera, Orrenius, Nilsson & Berggren, 1990). In addition, the NE, which has structural continuity with the endoplasmic reticulum (ER) (Franke, Scheer, Krohne & Jarasch, 1981) and contains Ca^{2+}-binding protein (Opas, Dziak, Fliegel & Michalak, 1991), may be a Ca^{2+} store. The ATP-dependent Ca^{2+} accumulation in NE, and IP_3- or cADPr-dependent Ca^{2+} release from NE to the nuclear matrix, were recently reported in isolated liver nuclei (Gerasimenko, Gerasimenko, Tepikin & Petersen, 1995). Biochemical studies showed that there are receptors for IP_3 or inositol 1,3,4,5-tetrakisphosphate on the nuclear membranes (Malviya, 1994). However, the *in vivo* mechanism of the regulation of $[Ca^{2+}]_n$ under physiological conditions still remains unclear. The only way to obtain conclusive evidence is to deliver Ca^{2+}-releasing reagents directly inside or outside the nucleus in intact cells.

Here we present the results of temporal and spatial analyses of $[Ca^{2+}]_n$ and $[Ca^{2+}]_c$ in immature hamster oocytes obtained using confocal fluorescence microscopy, combined with the techniques of the iontophoretic injection of charged reagents and the photolysis of caged compounds by UV irradiation (McCray & Trentham, 1989). Immature hamster oocytes show Ca^{2+} oscillations either spontaneously or in response to external stimuli, such as sperm, serotonin, or serum (Fujiwara, Nakada, Shirakawa & Miyazaki, 1993; Shiraishi *et al.* 1995). Each Ca^{2+} rise in the oscillations is based on IP_3-induced Ca^{2+} release (IICR) from intracellular stores (Fujiwara *et al.* 1993), and is frequently initiated in the cortical region near the nucleus, or germinal vesicle (GV) (Shiraishi *et al.* 1995). In mouse oocytes, similar IP_3-dependent spontaneous oscillations were also reported (Carroll & Swann, 1992), but the onset of each rise was synchronous over the oocyte (Carroll *et al.* 1994). The iontophoretic injection enabled us to deliver of IP_3 or Ca^{2+} focally, not only to the cytoplasm, but also to the nucleoplasm. The nucleus of immature hamster oocytes is as large as 20 μm in diameter and is located close to the plasma membrane, allowing impalement of the nucleus with a micropipette. Alternatively, UV irradiation of oocytes preloaded with caged IP_3 stimulates the entire oocyte simultaneously by a stepwise increase in IP_3 concentration. These results provide direct evidence that the elevation of $[Ca^{2+}]_n$ is predominantly due to Ca^{2+} influx from the cytoplasm, and that IICR from NE into the nucleoplasm does not contribute to this process.

METHODS

Materials

Full-grown GV stage oocytes of the golden hamster were prepared as described previously (Fujiwara *et al.* 1993). In short, animals were killed by cervical dislocation, and then oocytes collected from follicles were freed from surrounding cumulus cells and zona pellucidae by pipetting and trypsin (Gibco, Grand Island, NY, USA) treatment, respectively. Since hamster oocytes freed from cumulus cells undergo spontaneous maturation, all experimental procedures were completed within approximately 1 h after the removal of cumulus cells, during which most oocytes remained at the GV stage. The composition of the medium for oocyte preparation was (mM): NaCl, 94·6; KCl, 4·8; $CaCl_2$, 1·7; $MgSO_4$, 1·2; KH_2PO_4, 1·2; sodium lactate, 22; sodium pyruvate, 0·5; glucose, 5·6; $NaHCO_3$, 5·1; and Hepes, 19·4 (pH 7·4). The medium was supplemented with 4 mg ml^{-1} bovine serum albumin before use, except for the enzymatic treatment.

Ca^{2+} imaging with confocal microscopy

The strategy of ratiometric Ca^{2+} imaging with two Ca^{2+} indicators in the present study was basically similar to that described by Lipp & Niggli (1993), except that we used Calcium Green-1 (CG; hexapotassium salt, Molecular Probes) instead of Fluo-3. Fura Red (FR; tetraammonium salts, Molecular Probes), which has a longer emission wavelength and an inverse dependence on Ca^{2+} concentration ($[Ca^{2+}]$) compared with CG, was used as another Ca^{2+} indicator. After removal of the zona, oocytes were placed in a dish on an inverted microscope, and injected with about 10 pl (one-twentieth of the volume of oocytes) of injection solution containing (mM): CG, 0·6; FR, 3·0; and Hepes–KOH, 10 (pH 7·3). The final concentrations of dyes in oocytes, therefore, were calculated as approximately 30 and 150 μM, respectively. The dye injection was carried out in the normal medium, or in a medium supplemented with 10 μM thapsigargin (Sigma). Then the oocytes were transferred to the confocal laser scanning microscope (LSM310; Carl Zeiss, Oberkochen, Germany). Ca^{2+} imaging during iontophoretic injections or photolysis of caged IP_3 (see below) was carried out in Ca^{2+}-free medium, whose composition was (mM): NaCl, 117·5; KCl, 4·8; $MgSO_4$, 1·2; KH_2PO_4, 1·2; sodium lactate, 22; sodium pyruvate, 0·5; glucose, 5·6; and Hepes, 19·4 (pH 7·4). Temperature was kept at 31–33 °C. An Achroplan ×63 objective water immersion lens (NA 0·9; Carl Zeiss) was used for all experiments. The 488 nm argon laser was equipped for excitation, and the emitted fluorescence was split by a dichroic mirror (580 nm) after passing through the pinhole. These signals passed through a band-pass filter of 540 ± 25 nm and a long-pass filter of 590 nm, respectively, and were detected by separate photomultiplier tubes simultaneously. No significant cross-over between CG and FR signals was present in our experimental conditions. At the same time as the acquisition of fluorescence

signals, the transmitted light through the condenser was detected with another photomultiplier to obtain the differential interference contrast (DIC) images from the same focal plane as fluorescence images. The laser spot was scanned continuously at the rate of 0·19 s per image in a raster pattern, to acquire a series of 128 × 128 pixel 8-bit digital images, each of which was composed of three channels (CG, FR and DIC images). Fluorescence images of CG and FR were first low-pass filtered (3 × 3 or 5 × 5 pixel), the ratio was calculated in a pixel-to-pixel manner, and then a low-pass filter was applied on the ratio images again. In the line-scanning mode, the laser was repeatedly scanned on a fixed line at the rate of 2 ms per line, and line signals acquired were sequentially arranged to construct the line-scan images. Low-pass filter (7 × 7 pixel) was applied on the images before calculating the ratio. The acquisition and processing of images, and the measurement of fluorescence and ratio signals were all accomplished by custom macro programs using the functions supported by LSM software package (Carl Zeiss).

Iontophoretic injection

A glass micropipette was prepared by pulling a Pyrex glass tube (o.d. 1·4 mm, with microfilament inside) with the pipette puller (PA-81, Narishige, Tokyo, Japan), and was backfilled with either IP_3 (synthetic, potassium salt, Dojindo, Kumamoto, Japan) solution (0·5 mM IP_3, 140 mM KCl, 1 mM $MgSO_4$, 10 mM Hepes, pH 7·3) or Ca^{2+} solution (20 mM $CaCl_2$) containing detergent Nonidet P-40 (0·02%; Sigma). Pipettes filled with these solutions have electrical resistances of about 200 and 400 MΩ, respectively. Before the impalement of the oocyte, 2 nA of positive DC was applied to the pipette containing IP_3 using the current-clamp amplifier, in order to avoid the leakage of IP_3, which is negatively charged in the injection solution. The acquisition of sequential images was started after the impalement, and then a rectangular pulse of negative current (injection current) of 2–8 nA for 1 s was applied to drive IP_3 out of the pipette. For the injection of Ca^{2+}, the polarities of current were reversed: i.e. −2 and +8 nA for the leak prevention and injection currents, respectively; the duration of the injection current was usually 4 s. No increase in $[Ca^{2+}]$ was detected in the control experiment where current was applied to the oocyte through a pipette containing neither IP_3 nor Ca^{2+}.

Photolysis of caged IP_3 by UV irradiation

Caged IP_3 (D-*myo*-inositol 1,4,5-trisphosphate $P^{4(5)}$-1-(2-nitrophenyl)-ethyl ester) was purchased from Calbiochem and dissolved in 10 mM Hepes–KOH (pH 7·5). Oocytes were pre-injected with caged IP_3 together with CG and FR (0·4 mM caged IP_3, 0·4 mM CG, 2 mM FR in the pipette), giving a final concentration of approximately 30 μM in the oocyte. A 50 mW mercury lamp (Carl Zeiss) was used as UV source. The UV light was applied to the specimen through the condenser, and the duration of irradiation was regulated by a mechanical shutter. Since a mirror which directed UV light to the condenser was placed in the path of transmitted light, only fluorescence images could be recorded during the response to caged IP_3. Instead, DIC images of the oocyte were recorded before and after the acquisition of a series of fluorescence images, to identify the position of the nucleus.

Staining of ER by DiIC18

Staining of ER in oocytes by DiIC18 (1,1′-dioctadecyl-3,3,3′,3′-tetramethylindocarbocyanine perchlorate; Molecular Probes) was carried out as described elsewhere (Terasaki & Jaffe, 1991; Shiraishi *et al.* 1995). Briefly, live oocytes were injected with soy bean oil saturated with DiIC18, incubated for 15–30 min, and observed by confocal microscope with a 514 nm argon laser for excitation and a 590 nm long-pass filter for emission. Transmitted light images of the same focal plane used the 488 nm laser line and Nomarski microscope optics.

RESULTS

Distribution of fluorescence of Calcium Green and Fura Red in oocytes

When oocytes at the GV stage were injected with CG and FR, the fluorescence intensity of both dyes in the nucleus was higher than that in the cytoplasm in all cases (Fig. 1*B* and *C*). Such distribution of fluorescence is reasonable, since membranous structures which exclude the hydrophilic dyes are abundant in the cytoplasm, but not in the nucleus. The ratio of the fluorescence intensity, CG/FR, was almost uniform over the entire oocyte (Fig. 1*D*). The ratio values in

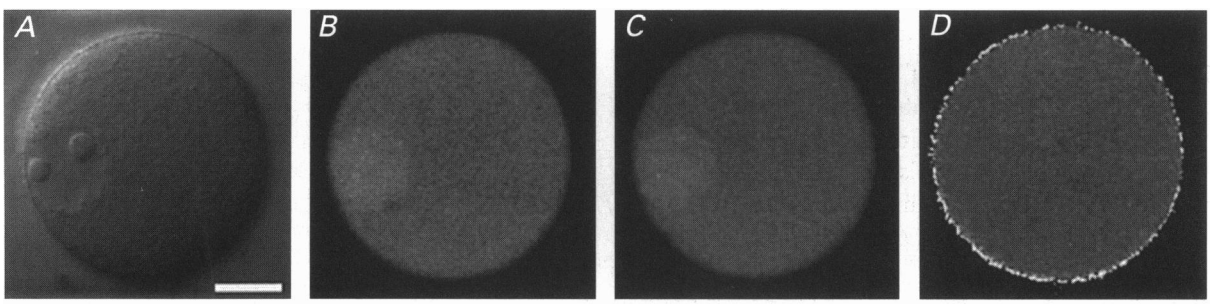

Figure 1. Bright field, fluorescence and ratio images of a hamster oocyte

The oocyte was pre-injected with both CG and FR, and observed with a 488 nm argon laser 10 min after injection. *A*, DIC image. The nucleus can be clearly identified at the 9 o'clock position with two nucleoli in it. *B* and *C*, fluorescence images of CG and FR, respectively. In both images, fluorescence in the nucleus was higher than that in other areas in the oocyte. *D*, the image of ratio values calculated in a pixel-to-pixel manner between *B* and *C*. The bright 'ring' in the periphery is an artifact. Intensities of transmitted and fluorescence signals as well as ratio values were digitized linearly in 8-bit. For ratio values, the minimum and maximum were 0·0 and 4·0, respectively. Scale bar is 20 μm.

both the nucleus (R_n) and cytoplasm (R_c) were not significantly different from 1 (1·04 ± 0·24 and 1·00 ± 0·25, respectively; mean ± S.D., $n = 27$), when the ratio of the concentration of injected dyes was 1 : 5 (CG : FR). The fact that the R_n/R_c ratio was very close to 1 (1·04 ± 0·06) indicates that the difference between $[Ca^{2+}]_n$ and $[Ca^{2+}]_c$ was negligible (see Discussion).

Ca^{2+} rise during Ca^{2+} injection

When Ca^{2+} was injected iontophoretically into the cytoplasm in the vicinity of the nucleus, a Ca^{2+} rise was detected at the injection site immediately after the onset of injection, and spread through both cytoplasm and nucleoplasm (Fig. 2*A*). The rate of rise in $[Ca^{2+}]_n$, however, was apparently slower than that in $[Ca^{2+}]_c$ (Fig. 3*A*). Conversely, when Ca^{2+} was injected directly into the nucleus, the rise in $[Ca^{2+}]_c$ delayed compared with that in $[Ca^{2+}]_n$ (Figs 2*B* and 3*B*). Such a delay in diffusion at the boundary between the nucleus and cytoplasm was also apparent in Fig. 3*C* and *D*, which shows one-dimensional spatial profiles of the CG/FR ratio at a time point during the rising phase. These results indicate that the NE works as a substantial barrier to Ca^{2+} diffusion. It was not a strong barrier, however, since both $[Ca^{2+}]_n$ and $[Ca^{2+}]_c$ reached a plateau of the same level within about 2 s after the onset of Ca^{2+} injection (Fig. 3*A* and *B*), and, therefore, the nucleus seemed not to be isolated from cytoplasmic changes in Ca^{2+}. The R_n/R_c ratios were 1·00 ± 0·07 and 1·04 ± 0·10 ($n = 12$) before injection and at the plateau of the response, respectively. Furthermore, the rate of CG/FR rise at the injection site was similar in cyto- and nucleoplasmic Ca^{2+} injections, suggesting that Ca^{2+} buffering in the nucleoplasm is comparable to that in the cytoplasm. The overall similarity between the time courses of the spread of Ca^{2+} across the NE in both directions suggested that NE had no rectifying property for the diffusion of Ca^{2+}. The treatment with thapsigargin, which is an inhibitor of the Ca^{2+} pump of the ER (Thastrup, Cullen, Drøbak, Hanley & Dawson, 1990), and probably also of the NE (Lanini, Bachs & Carafoli, 1992), resulted in an elevated CG/FR ratio in both the nucleus and cytoplasm at the resting state ($R_n = 1·39 \pm 0·18$, $R_c = 1·39 \pm 0·24$, $n = 7$), as expected from the inhibitory effect of thapsigargin on Ca^{2+} uptake into Ca^{2+} stores. However, the R_n/R_c ratio did not deviate from 1 either at the resting state or at the plateau phase during Ca^{2+} injection (0·98 ± 0·08 and 0·96 ± 0·08, respectively, $n = 5$). This indicates that active Ca^{2+} transport by the Ca^{2+} pump does not participate in the maintenance of the steady-state balance between $[Ca^{2+}]_n$ and $[Ca^{2+}]_c$. All of these results led us to characterize the nucleus as a passive structure whose Ca^{2+} concentration is not regulated independently from the cytoplasm either at the resting or elevated state.

Structure of the ER around the nucleus

As we have reported previously, hamster oocytes at the GV stage have several clusters of ER located on the inner surface of plasma membrane, and one or two of them are close to the nucleus (Shiraishi *et al.* 1995). DiIC18, a lipophilic dye which can be applied by an oil drop method to preferentially label the ER (Terasaki & Jaffe, 1991), stained the ER cluster beside the nucleus as a bright oval structure as shown in Fig. 4*B*. The fact that the ER cluster was easily identified as a relatively smooth area in a DIC image as well (Fig. 4*A*), enabled us to examine the Ca^{2+} dynamics in relation to the position of ER clusters without any staining procedure for ER (see below). The NE was lined with a DiIC18-positive structure, which had continuity with the thin meshwork in the surrounding cytoplasm (Fig. 4*C* and *D*). This perinuclear structure, possibly stacks of ER, is likely to serve as Ca^{2+}-releasable stores in response to IP_3, because the IP_3 receptors have been detected on the boundary of the nucleus by immunohistochemical staining, although less intensely than in ER clusters (Shiraishi *et al.* 1995).

Ca^{2+} rise induced by IP_3 injection

We next examined the distribution of IICR inside and outside the nucleus by injecting IP_3 directly into the cytoplasm or nucleoplasm. When a small amount of IP_3

Figure 2. Ca^{2+} rise in response to Ca^{2+} or IP_3 injection

All images, except the first ones in each series, are ratio (CG/FR) images, presented with pseudocolour. Images were acquired at 0·19 s intervals; every other image is shown. Colour scale is common to all series of images in this figure, and also to Fig. 6. Ratio images are overlaid with white line drawings which show the boundaries of oocytes and nuclei, and the position of the micropipette inserted for iontophoretic injection of Ca^{2+} or IP_3. *A* and *B*, responses to cytoplasmic and nucleoplasmic injection of Ca^{2+}, respectively. In both cases, Ca^{2+} was injected with 8 nA positive current for 4 s. *C* and *D*, responses to the IP_3 injection into the cytoplasm in the vicinity of the nucleus. Injection current was −2 nA in *C* and −5 nA in *D* for 1 s. *E*, response to nucleoplasmic IP_3 injection with −8 nA for 1 s. *F*, response to IP_3 injected beside the ER cluster (−5 nA, 1 s). The ER cluster can be seen as a 'smooth' region in the DIC image (arrowhead, see also Fig. 4). The nucleus was associated with this ER cluster, but not seen in this image because it was located below the focal plane. Dashed lines in ratio images in *F* indicate the outline of the ER cluster. Each image represents 33 × 33 μm^2 (*A*–*E*) or 50 × 50 μm^2 (*F*).

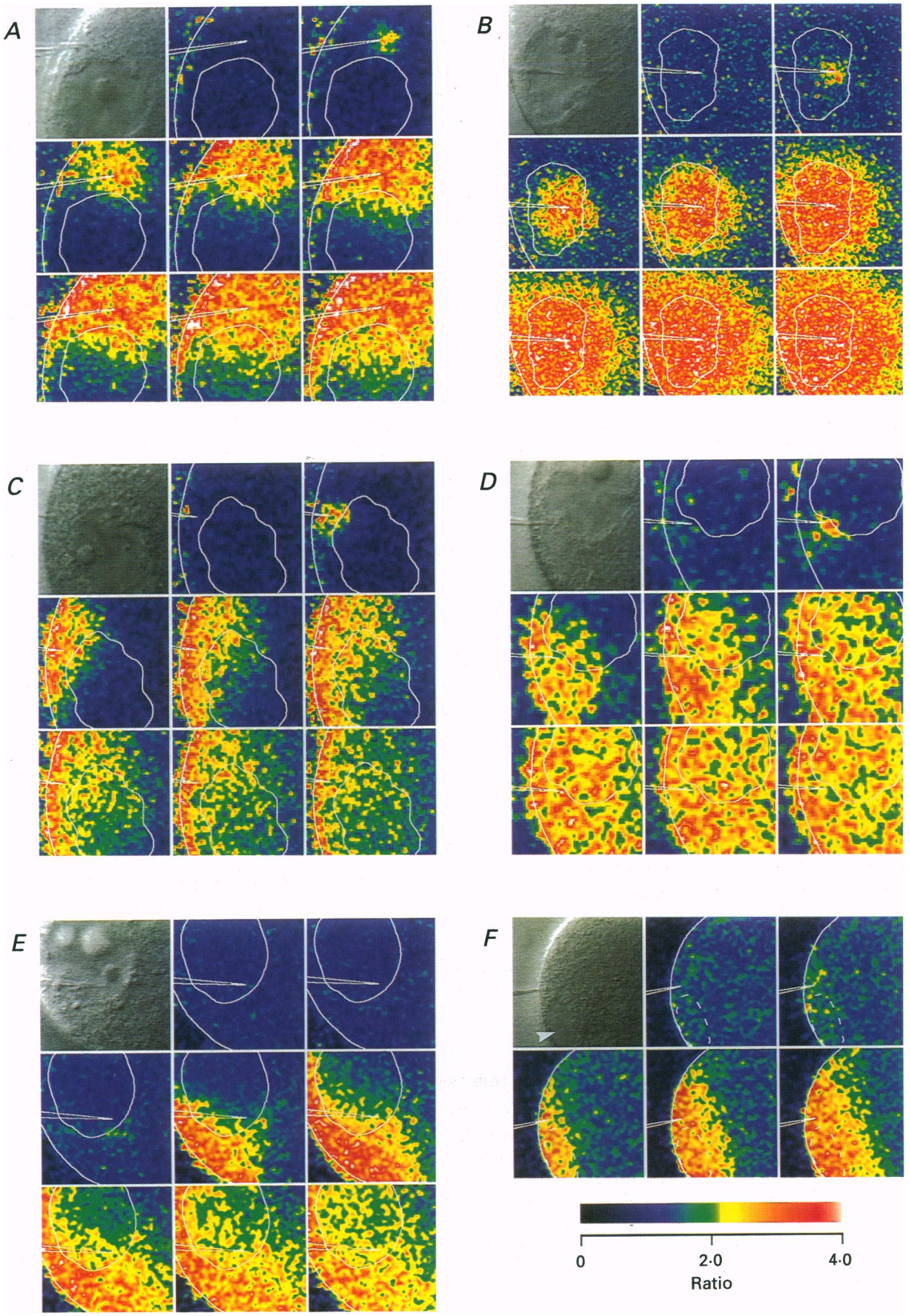

Figure 2. For legend see facing page.

was injected with an injection current of −2 nA for 1 s into the cytoplasmic space between the plasma membrane and the nucleus, a Ca^{2+} rise rapidly propagated laterally along the plasma membrane, but attenuated in the nucleus as seen in the lower plateau level of CG/FR ratio (Figs 2*C* and 5*A*). This amount of IP_3 is large enough to induce a Ca^{2+} wave which regeneratively propagates over the entire cytoplasm in mature hamster eggs (Miyazaki *et al.* 1992). The regenerative Ca^{2+} wave was not produced in immature oocytes, probably because ER and IP_3 receptors are distributed only sparsely in the interior cytoplasm (Shiraishi *et al.* 1995). A larger rise in Ca^{2+} which spread into the deeper cytoplasm was induced by the injection of a larger amount of IP_3 (−5 nA, 1 s; Fig. 2*D*), and it was not attenuated in the nucleus (Fig. 5*B*). The delay between the rises in $[Ca^{2+}]_n$ and $[Ca^{2+}]_c$ was apparent (Fig. 5*B*), although it was shorter than that detected during Ca^{2+} injections (Fig. 3*A*). A regenerative wave was still not induced by this amount of IP_3, and the Ca^{2+} rise was attenuated in the centre and opposite side of the cytoplasm (not shown in Fig. 2*D*).

When a still larger amount of IP_3 (−8 nA, 1 s) was delivered in close proximity to the inner surface of the NE, a small Ca^{2+} rise was initially detected *outside* rather than *inside* the nucleus (see second and third ratio images in Fig. 2*E*, and arrow in Fig. 5*C*). The following large increase in $[Ca^{2+}]$, which also occurred first in the cytoplasm, propagated mainly along the plasma membrane and, to a lesser extent, into the nucleus. These results strongly indicated the functional absence of IICR from the inner face of NE; i.e. even in the case where the IP_3 concentration in the nucleus is preferentially increased, IP_3 will diffuse out of the nucleus to the cytosol and induce Ca^{2+} release

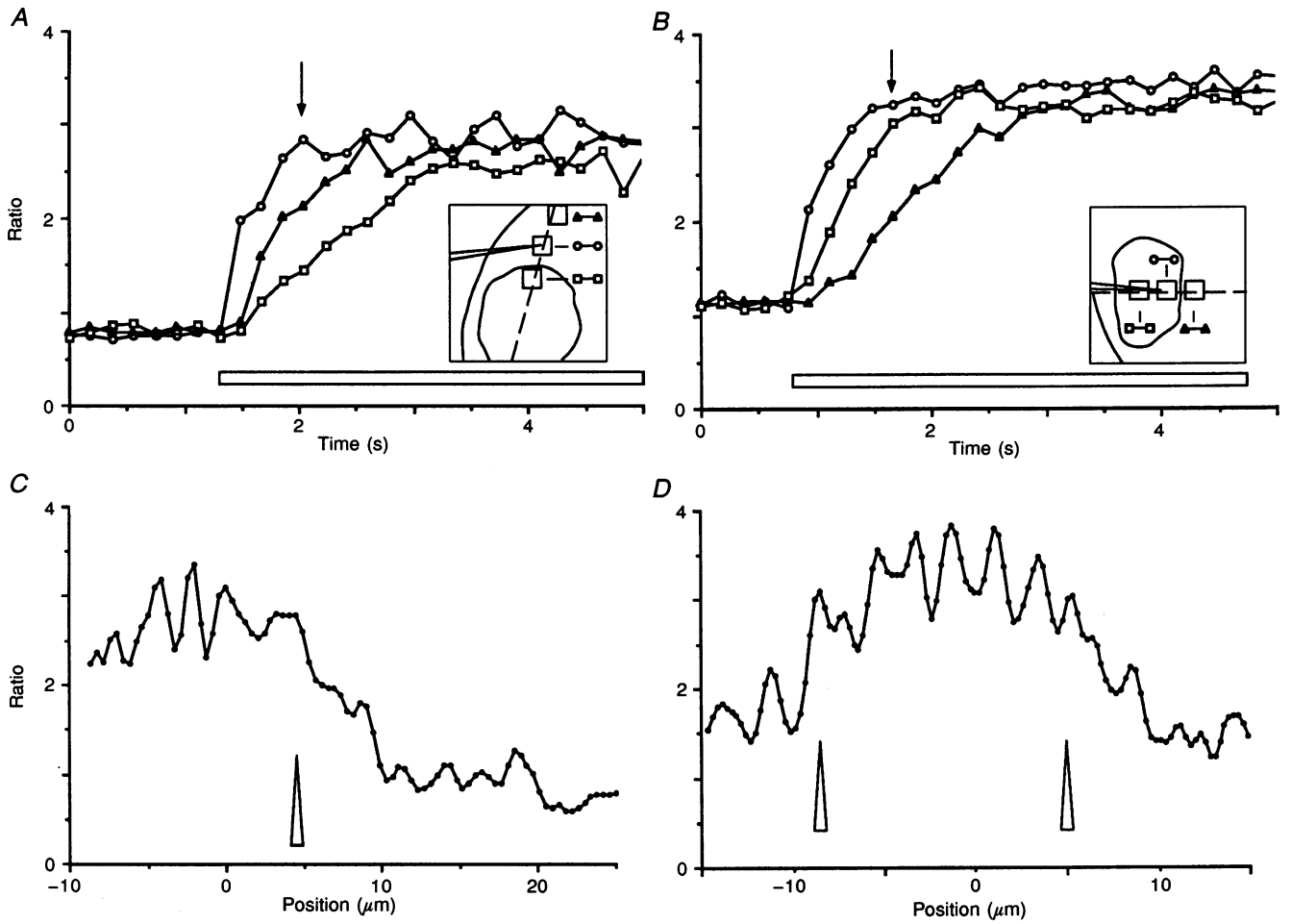

Figure 3. Time course and spatial profile of the Ca^{2+} rise during Ca^{2+} injection

A and *B*, Ca^{2+} rise during cyto- and nucleoplasmic Ca^{2+} injection (same responses as Fig. 2*A* and *B*), respectively. Ratio values were averaged in squares of $7 \times 7\ \mu m^2$ at the injection site (○), and at cytoplasmic (△) and nucleoplasmic (□) sites equidistant from the injection site, as shown in the insets. The horizontal bar indicates the period of Ca^{2+} injection. *C* and *D*, one-dimensional spatial profile at a time point during the rising phase of *A* and *B*. The corresponding time point and the position of line are indicated by arrows in the graphs and dashed lines in the insets of *A* and *B*. The position of the tip of the injection pipette was taken as zero position. Thin triangles indicate the position of the NE.

from the perinuclear ER and the ER cluster. Subsequently the released Ca^{2+} diffused into the nucleus, resulting in an increase in $[Ca^{2+}]_n$.

Ca^{2+} rise induced by photolysis of caged IP_3

The spatial and temporal pattern of Ca^{2+} rise in response to a sudden increase of IP_3 concentration in the whole oocyte was investigated by irradiating UV light on an oocyte preloaded with caged IP_3, instead of focal IP_3 application by iontophoretic injection. The $[Ca^{2+}]$ increase was initiated in the cortical region beside the nucleus in all oocytes examined (Fig. 6*A*, $n = 9$). When the Ca^{2+} response was recorded at the focal plane which included the ER cluster beside the nucleus, the Ca^{2+} rise in the perinuclear ER region preceded that in other regions (Fig. 6*B*), indicating that it can be a 'hot spot' of IICR. The ER clusters other than the one beside the nucleus may be additional hot spots, since the Ca^{2+} rise was occasionally initiated at two or three distinct areas, all of which were located in the cortical region (data not shown). The idea that the ER cluster is more sensitive to IP_3 than other areas was further supported by the observation of preferential Ca^{2+} release at the ER cluster in response to the IP_3 injection adjacent to the cluster (Fig. 2*F*). The high sensitivity of the ER cluster may be explained simply by the high density of IP_3-sensitive Ca^{2+} stores there, which is a favourable condition to produce a regenerative burst on the basis of the sensitization of IICR by cytoplasmic Ca^{2+} (Iino & Endo, 1992).

The increase in $[Ca^{2+}]_n$ was always delayed with respect to that in $[Ca^{2+}]_c$ around the nucleus, as shown in the consecutive two-dimensional images in Fig. 6*A* and *B*. This delay was clearly detected in the high-time resolution line-scan image in Fig. 6*C*. These results further supported the conclusion that Ca^{2+} is not released inside the nucleus. In addition to the major $[Ca^{2+}]_c$ rise beneath the plasma membrane, a small but significant rise was detected in the perinuclear region (Fig. 6*A*, arrowhead). This probably reflected IICR from the perinuclear ER. The rapid equilibration of $[Ca^{2+}]_n$ with $[Ca^{2+}]_c$, following stimulation with caged IP_3, compared with the response to the injection of Ca^{2+} or IP_3 (Fig. 2), may be due to the effective recruitment of the perinuclear Ca^{2+} stores by elevation of the IP_3 concentration all around the nucleus, and subsequent massive influx through the NE.

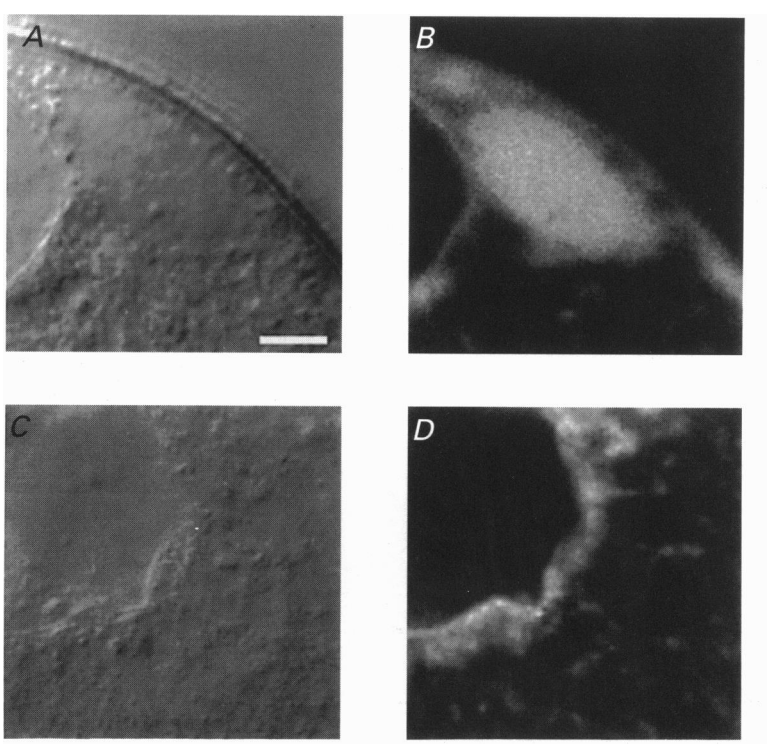

Figure 4. The ER around the nucleus

A and *C*, DIC images, and *B* and *D*, corresponding images of DiIC18 fluorescence. Scale bar is 5 μm. Images were recorded 20–30 min after DiIC18 injection. A relatively smooth region can be seen in the DIC image (*A*) at the position where DiIC18 fluorescence is concentrated (*B*). The NE of the same oocyte was surrounded by a DiIC18-positive structure, which was connected with a fine meshwork in the cytoplasm (*D*). The fluorescence signal was highly amplified during the acquisition of the image in *D*, to highlight the fine structure around the nucleus. Actual fluorescence of the perinuclear ER was much less intense than that of the ER cluster in *B*.

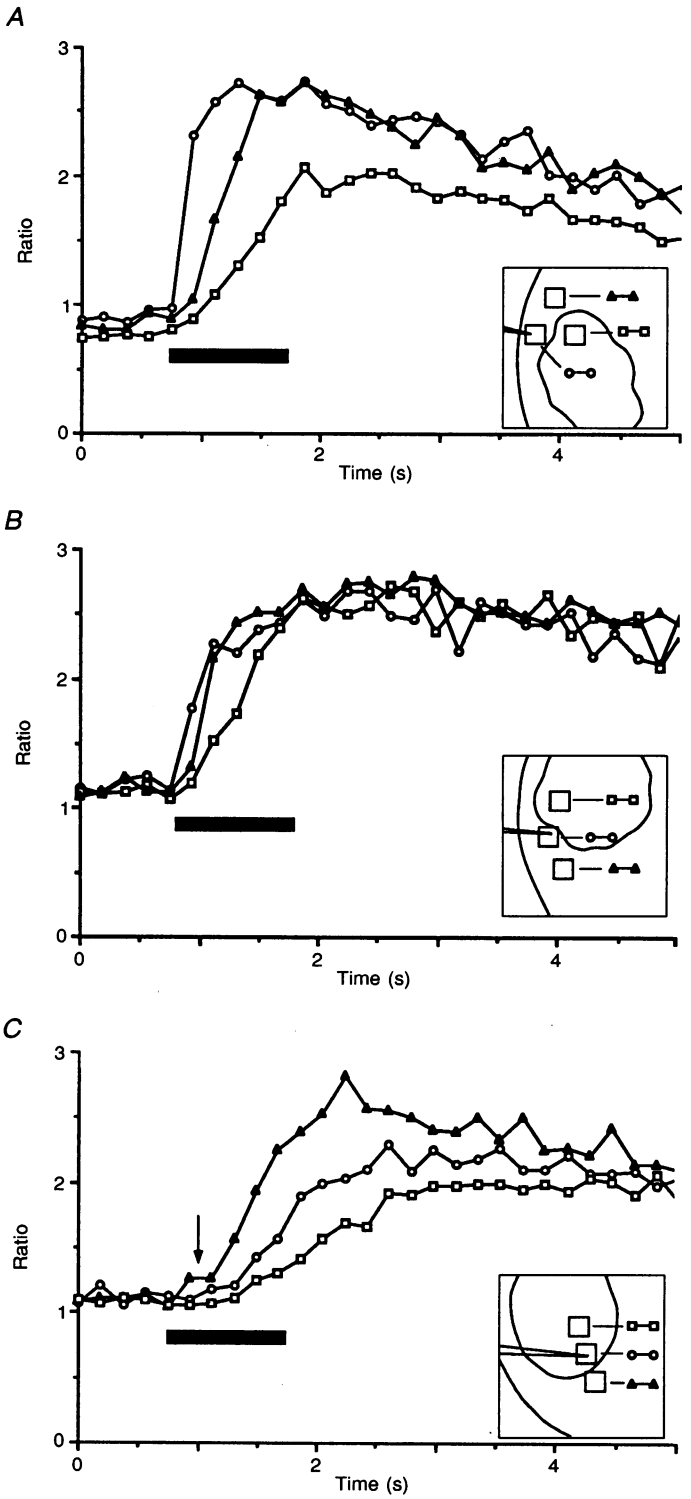

Figure 5. Time course of the Ca^{2+} rise in response to IP_3 injection

A and *B*, responses to low and high dose of IP_3 injected into cytoplasm (same responses as in Fig. 2*C* and *D*). *C*, response to nucleoplasmic injection (same response as in Fig. 2*E*). The injection period is indicated by the bar. Ratio values were averaged in a similar manner as in Fig. 3, and areas for calculation are indicated in the insets. The arrow in *C* indicates the initial small rise detected outside the nucleus.

DISCUSSION

Ca^{2+} imaging with two dyes and the distribution of $[Ca^{2+}]$ in hamster oocytes

We applied confocal fluorescence microscopy in the analysis of Ca^{2+} dynamics in hamster oocytes, using two fluorescent Ca^{2+} indicators, CG and FR, which are excitable by visible laser and have similar Ca^{2+} dissociation constants. For the purpose of the present study, the primary importance was to detect the spatiotemporal changes in $[Ca^{2+}]$, rather than to measure the absolute value of the concentration. Uniformity of CG/FR ratio between the nucleus and cytoplasm was beneficial to compare the time course of Ca^{2+} rise in these compartments. Since the distribution of fluorescence remained essentially unchanged during the incubation for at least 40 min after the injection of dyes, it is credible that the changes in the CG/FR ratio in the present study reflected the changes in $[Ca^{2+}]$. Dual-emission ratio imaging with indo-1 using a UV-laser confocal

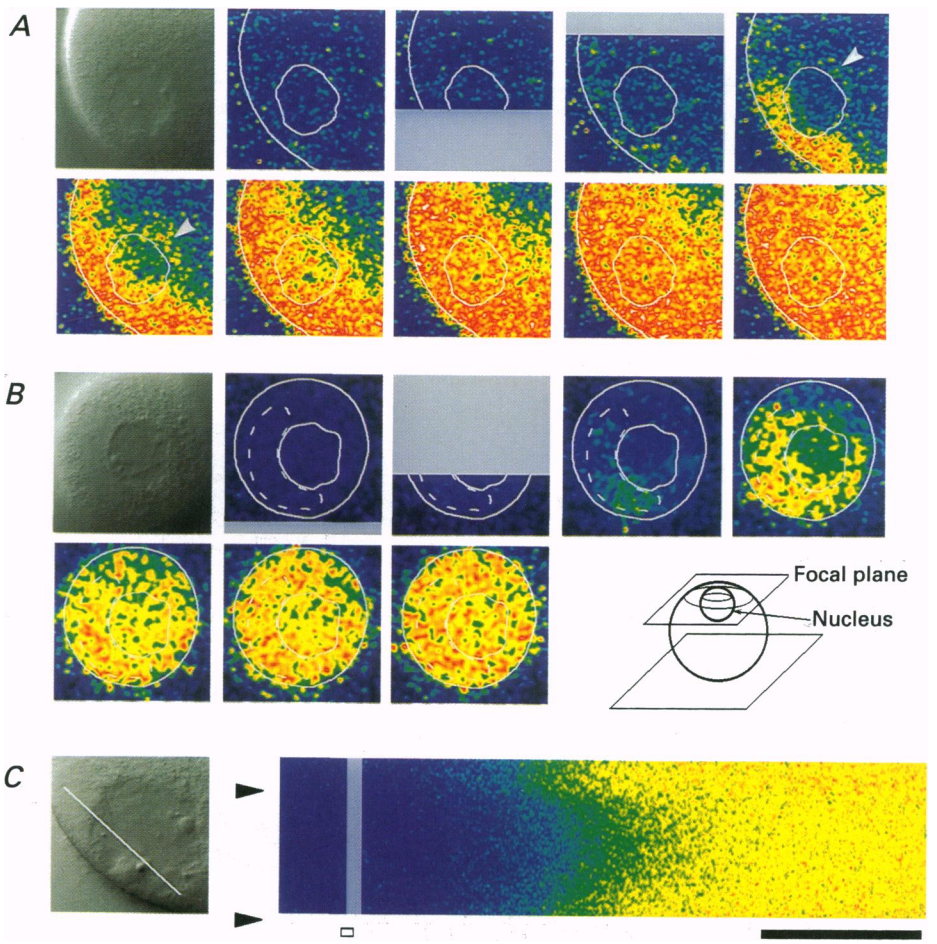

Figure 6. The Ca^{2+} rise in response to photolysis of caged IP_3

UV light from a mercury lamp was applied to the oocytes preloaded with about 30 μM caged IP_3. *A*, oocyte was irradiated uniformly for 0·1 s. Ca^{2+} release in perinuclear region opposite to the plasma membrane is indicated by arrowheads. *B*, the nucleus was located in the top of the oocyte, and the focal plane was set about 10 μm below the upper end of the oocyte, as shown in the inset. A large ER cluster encircled the left to the bottom of the nucleus. Dashed lines in ratio images indicate the outlines of the ER cluster. The interval of images is 0·19 s for both *A* and *B*. Measurement could not be made during UV irradiation, since the strong light was contaminated in both fluorescence-detectors. Grey areas (from the middle of the second ratio image to the top of the third in *A*, and from the bottom of the first ratio image to the middle of the second in *B*) indicate the period, not region, of irradiation, because each image was constructed from fluorescence signals excited by raster scanning of a laser spot in top–down direction. *C*, line-scan image (right) was obtained by scanning lasers at the rate of 2 ms per line on a line crossing the nucleus, as indicated by the white line in the DIC image (left). A series of one-dimensional ratio values were successively aligned horizontally. Arrowheads indicate the position of NE. Open bar indicates the period of irradiation. Filled bar is 1 s. Each image represents 50 × 50 μm^2 (*A*), 56 × 56 μm^2 (*B*) or 33 × 33 μm^2 (DIC image in *C*).

microscope seems to be the best method for the quantitative Ca^{2+} imaging at present. Nevertheless, compared with this method, ratio imaging with CG and FR has the following advantages: (1) better signal-to-noise ratio due to stronger fluorescence signals; (2) less cytotoxicity of visible laser, compared with UV laser; (3) combination with caged compounds; and (4) simultaneous recording with bright field images from the same focal plane.

Although we did not calibrate $[Ca^{2+}]_n$ and $[Ca^{2+}]_c$ in absolute terms, the fact that the CG/FR ratio in the nucleus was very similar to that in the cytoplasm indicates that there is no significant difference between $[Ca^{2+}]_n$ and $[Ca^{2+}]_c$. This view was supported by several lines of evidence. First, thapsigargin did not affect the R_n/R_c ratio either at the resting or elevated state, suggesting that the active Ca^{2+} transport by the Ca^{2+} pump is unlikely to play a role in maintaining the balance between $[Ca^{2+}]_n$ and $[Ca^{2+}]_c$. Second, Ca^{2+} can diffuse across the NE relatively freely (see below), and no rectification in the direction of diffusion was present. Third, oocytes which were loaded with fura-2 showed an equal fluorescence ratio in the nucleus and cytoplasm, when excited by UV light of 340 and 380 nm and observed with a ×100 NA 1·3 objective lens using conventional fluorescence microscopy (authors' unpublished data).

Source of Ca^{2+} in the nucleus

The present study provided detailed information about the site of IICR, which leads to a rise in $[Ca^{2+}]_n$ of hamster oocytes *in vivo*. Hennager, Welsh & DeLisle (1995) reported an increase in $[Ca^{2+}]_n$ induced by intranuclear IP_3 injection in *Xenopus* oocytes. Although its resistance to the presence of heparin, the inhibitor of IICR, in the cytoplasm suggested that it was probably due to Ca^{2+} release directed inside the nucleus, little spatial and temporal information about the relation between $[Ca^{2+}]_n$ and $[Ca^{2+}]_c$ was provided. In hamster oocytes, the ER cluster(s) beside the nucleus probably stores a large amount of releasable Ca^{2+} and serves as the major source of Ca^{2+} around and inside the nucleus. The perinuclear ER is also likely to make a significant contribution to the rise in $[Ca^{2+}]_n$. Even if the amount of Ca^{2+} released in the cytoplasm from the perinuclear ER is small, it may effectively diffuse into the nucleus and facilitate the equilibration of $[Ca^{2+}]_n$ with $[Ca^{2+}]_c$. In isolated rat liver nuclei, cADPr as well as IP_3 evoked Ca^{2+} release from the NE into the nucleoplasm (Gerasimenko *et al.* 1995). Any Ca^{2+} increase by nucleo- or cytoplasmic injection of cADPr was not detected either in the nucleus or cytoplasm in our preliminary experiments with intact hamster oocytes (data not shown). The contradiction with the result of studies with isolated liver nuclei may be due to the difference of cell types. It must be noted, however, that the topology of the NE and the associated perinuclear structures was preserved well in our experimental system when compared with isolated nuclei. As a whole, the present results indicate that the source of Ca^{2+} increase in the nucleus of the hamster oocyte is not Ca^{2+} released directly to the nucleoplasm from the NE, but Ca^{2+} which is initially released from the ER into the cytoplasm.

The NE acts as a substantial diffusion barrier for Ca^{2+} as shown in experiments in which Ca^{2+} was injected in close proximity to the inner or outer surface of the NE (Fig. 2*A* and *B*), but its effect seems to be functionally negligible in terms of the time course of the physiological responses in oocytes. Ca^{2+} ions diffuse in and out of the nucleus probably through the nuclear pore, which is thought to be highly permeable for small molecules (Horowitz, 1972). The basic property of the NE of GV, which is an unusually large nucleus in oocytes, may be similar to that of the nucleus in somatic cells, and the rate of Ca^{2+} diffusion across the NE seemed to be fast in general, as suggested by the fast equilibration of $[Ca^{2+}]_n$ with $[Ca^{2+}]_c$ in the Ca^{2+} responses in oocytes with GV (Carroll *et al.* 1994; Gillot & Whitaker, 1994), as well as in many somatic cells (Giovannardi, Cesare & Peres, 1994; Lin *et al.* 1994; O'Malley, 1994; Minamikawa *et al.* 1995). Al-Mohanna *et al.* (1994) reported that a relatively large $[Ca^{2+}]_c$ rise (> 300 nM) induced by depolarization in neurons was attenuated in the nucleus, while the attenuation was not observed in our experiments of Ca^{2+} injection (Fig. 3*A* and *B*). The apparent discrepancy is probably attributable to the difference in the time course of $[Ca^{2+}]_c$ changes. The duration of depolarization-induced $[Ca^{2+}]_c$ rise was very short in their experiments and $[Ca^{2+}]_c$ declined before the equilibration with $[Ca^{2+}]_n$. However, it is predicted that, had $[Ca^{2+}]_c$ been kept elevated for as long as 2 or 3 s, $[Ca^{2+}]_n$ would also have reached a peak level as high as that of $[Ca^{2+}]_c$.

Immature hamster oocytes show spontaneous Ca^{2+} oscillations. Although its physiological significance in the context of oocyte maturation is still unclear, it is apparently due to Ca^{2+} release through IP_3 receptors, since it was completely blocked by a function-inhibiting monoclonal antibody to the IP_3 receptor (Fujiwara *et al.* 1993). In addition, each rise in the oscillations was frequently initiated in the region close to the nucleus (Shiraishi *et al.* 1995). The preferential production of IP_3 around and/or in the nucleus might trigger Ca^{2+} rises at this region during oscillations. The presence of enzymes involved in phosphoinositide metabolism in the nucleus has been shown in other cell types (Divecha, Rhee, Letcher & Irvine, 1993). We suppose, however, from the present results of the experiment with caged IP_3 that the ER cluster, which is more sensitive to IP_3 than other areas in the oocyte, can act as a trigger zone, when IP_3 concentration is uniform over the oocyte.

Role of Ca^{2+} in the nucleus

At present, the role of intranuclear Ca^{2+} in mammalian oocytes at the GV stage is unknown. One possibility is its involvement in the regulation of GV breakdown (GVBD).

Several lines of evidence suggested the role of Ca^{2+} in GVBD in bovine (Homa, 1991), pig (Kaufman & Homa, 1993), and mouse (Lefèvre *et al.* 1995) oocytes, whereas others reported the lack of dependence of GVBD on Ca^{2+} in mouse oocytes (Carroll & Swan, 1992; Tombes *et al.* 1992). The level of Ca^{2+} in the nucleus may be important for the regulation of nuclear events other than GVBD, such as the changes in chromatin structure. Although the significance of intranuclear Ca^{2+} during meiotic maturation of hamster oocytes should be clarified by future investigations, the present study provides insights about mechanisms regulating $[Ca^{2+}]_n$ not only in oocytes but also in somatic cells.

Al-Mohanna, F. A., Caddy, K. W. T. & Bolsover, S. R. (1994). The nucleus is insulated from large cytosolic calcium ion changes. *Nature* **367**, 745–750.

Baitinger, C., Alderman, J., Poenie, M., Schulman, H. & Steinhardt, R. A. (1990). Multifunctional Ca^{2+}/calmodulin-dependent kinase is necessary for nuclear envelope breakdown. *Journal of Cell Biology* **111**, 1763–1773.

Boynton, A. L., Whitfield, F. J. & MacManus, J. L. (1980). Calmodulin stimulates DNA synthesis by rat liver cells. *Biochemical and Biophysical Research Communications* **95**, 745–749.

Carroll, J. & Swann, K. (1992). Spontaneous cytosolic calcium oscillations driven by inositol trisphosphate occur during *in vitro* maturation of mouse oocytes. *Journal of Biological Chemistry* **267**, 11196–11201.

Carroll, J., Swann, K., Whittingham, D. & Whitaker, M. (1994). Spatiotemporal dynamics of intracellular Ca^{2+} oscillations during the growth and meiotic maturation of mouse oocytes. *Development* **120**, 3507–3517.

Divecha, N., Rhee, S.-G., Letcher, A. J. & Irvine, R. F. (1993). Phosphoinositide signalling enzymes in rat liver nuclei: phosphoinositidase C isoform $\beta 1$ is specifically, but not predominantly, located in the nucleus. *Biochemical Journal* **289**, 617–620.

Franke, W. W., Scheer, U., Krohne, G. & Jarasch, E.-D. (1981). The nuclear envelope and the architecture of the nuclear periphery. *Journal of Cell Biology* **91**, 39–50s.

Fujiwara, T., Nakada, K., Shirakawa, H. & Miyazaki, S. (1993). Development of inositol trisphosphate-induced calcium release mechanism during maturation of hamster oocytes. *Developmental Biology* **156**, 69–79.

Furuno, T., Hamano, T. & Nakanishi, M. (1993). Receptor-mediated calcium signal playing a nuclear third messenger in the activation of antigen-specific B cells. *Biophysical Journal* **64**, 665–669.

Gerasimenko, O. V., Gerasimenko, J. V., Tepikin, A. V. & Petersen, O. H. (1995). ATP-dependent accumulation and inositol trisphosphate- or cyclic ADP-ribose-mediated release of Ca^{2+} from the nuclear envelope. *Cell* **80**, 439–444.

Gillot, I. & Whitaker, M. (1994). Calcium signals in and around the nucleus in sea urchin eggs. *Cell Calcium* **16**, 269–278.

Giovannardi, S., Cesare, P. & Peres, A. (1994). Rapid synchrony of nuclear and cytosolic Ca^{2+} signals activated by muscarinic stimulation in the human tumour line TE571/RD. *Cell Calcium* **16**, 491–499.

Hennager, D. J., Welsh, M. J. & DeLisle, S. (1995). Changes in either cytoplasmic or nucleoplasmic inositol 1,4,5-trisphosphate levels can control nuclear Ca^{2+} concentration. *Journal of Biological Chemistry* **270**, 4959–4962.

Himpens, B., De Smedt, H. & Casteels, R. (1994). Relationship between $[Ca^{2+}]$ changes in nucleus and cytosol. *Cell Calcium* **16**, 239–246.

Homa, S. T. (1991). Neomycin, an inhibitor of phosphoinositide hydrolysis, inhibits the resumption of bovine oocyte spontaneous meiotic maturation. *Journal of Experimental Zoology* **258**, 95–103.

Horowitz, S. B. (1972). The permeability of the amphibian oocyte nucleus, *in situ*. *Journal of Cell Biology* **54**, 609–625.

Iino, M. & Endo, M. (1992). Calcium-dependent immediate feedback control of inositol 1,4,5-trisphosphate-induced Ca^{2+} release. *Nature* **360**, 76–78.

Katagiri, S., Takamatsu, T., Minamikawa, T. & Fujita, S. (1993). Secretogogue-induced calcium wave shows higher and prolonged transients of nuclear calcium concentration in mast cells. *FEBS Letters* **334**, 343–346.

Kaufman, M. L. & Homa, S. T. (1993). Defining a role for calcium in the resumption and progression of meiosis in the pig oocyte. *Journal of Experimental Zoology* **265**, 69–76.

Lanini, L., Bachs, O. & Carafoli, E. (1992). The calcium pump of the liver nuclear membrane is identical to that of endoplasmic reticulum. *Journal of Biological Chemistry* **267**, 11548–11552.

Lefèvre, B., Pesty, A. & Testart, J. (1995). Cytoplasmic and nucleic calcium oscillations in immature mouse oocytes: Evidence of wave polarization by confocal imaging. *Experimental Cell Research* **218**, 166–173.

Lin, C., Hajnóczky, G. & Thomas, A. P. (1994). Propagation of cytosolic calcium waves into the nuclei of hepatocytes. *Cell Calcium* **16**, 247–258.

Lipp, P. & Niggli, E. (1993). Ratiometric confocal Ca^{2+}-measurements with visible wavelength indicators in isolated cardiac myocytes. *Cell Calcium* **14**, 350–372.

McCray, J. A. & Trentham, D. R. (1989). Properties and uses of photoreactive caged compounds. *Annual Review of Biophysics and Biophysical Chemistry* **18**, 239–270.

Malviya, A. N. (1994). The nuclear inositol 1,4,5-trisphosphate and inositol 1,3,4,5-tetrakisphosphate receptors. *Cell Calcium* **16**, 301–313.

Minamikawa, T., Takahashi, A. & Fujita, S. (1995). Differences in features of calcium transients between the nucleus and the cytosol in cultured heart muscle cells: analyzed by confocal microscopy. *Cell Calcium* **17**, 165–176.

Miyazaki, S., Yuzaki, M., Nakada, K., Shirakawa, H., Nakanishi, S., Nakade, S. & Mikoshiba, K. (1992). Block of Ca^{2+} wave and Ca^{2+} oscillation by antibody to the inositol 1,4,5-trisphosphate receptor in fertilized hamster eggs. *Science* **257**, 251–255.

Nicotera, P., Orrenius, S., Nilsson, T. & Berggren, P.-O. (1990). An inositol 1,4,5-trisphosphate-sensitive Ca^{2+} pool in liver nuclei. *Proceedings of National Academy of Sciences of the USA* **87**, 6858–6862.

Nicotera, P., Zhivotovsky, B. & Orrenius, S. (1994). Nuclear calcium transport and the role of calcium in apoptosis. *Cell Calcium* **16**, 279–288.

O'Malley, D. M. (1994). Calcium permeability of the neuronal nuclear envelope: evaluation using confocal volumes and intracellular perfusion. *Journal of Neuroscience* **14**, 5741–5758.

Opas, M., Dziak, E., Fliegel, L. & Michalak, M. (1991). Regulation of expression and intracellular distribution of calreticulin, a major calcium binding protein of nonmuscle cells. *Journal of Cellular Physiology* **149**, 160–171.

Roche, E. & Prentki, M. (1994). Calcium regulation of immediate-early response genes. *Cell Calcium* **16**, 331–338.

Shen, S. S. & Buck, W. R. (1993). Sources of calcium in sea urchin eggs during the fertilization response. *Developmental Biology* **157**, 157–169.

Shiraishi, K., Okada, A., Shirakawa, H., Nakanishi, S., Mikoshiba, K. & Miyazaki, S. (1995). Developmental changes in the distribution of the endoplasmic reticulum and inositol 1,4,5-trisphosphate receptors and the spatial pattern of Ca^{2+} release during maturation of hamster oocytes. *Developmental Biology* **170**, 594–606.

Stricker, S. A., Centonze, V. E. & Melendez, R. F. (1994). Calcium dynamics during starfish oocyte maturation and fertilization. *Developmental Biology* **166**, 34–58.

Sullivan, K. M. C., Busa, W. B. & Wilson, K. L. (1993). Calcium mobilization is required for nuclear vesicle fusion *in vitro*: Implications for membrane traffic and IP_3 receptor function. *Cell* **73**, 1411–1422.

Terasaki, M. & Jaffe, L. A. (1991). Organization of the sea urchin egg endoplasmic reticulum and its reorganization at fertilization. *Journal of Cell Biology* **114**, 929–940.

Thastrup, O., Cullen, P. J., Dørbak, B. K., Hanley, M. R. & Dawson, A. P. (1990). Thapsigargin, a tumor promoter, discharges intracellular Ca^{2+} stores by specific inhibition of the endoplasmic reticulum Ca^{2+}-ATPase. *Proceedings of National Academy of Sciences of the USA* **87**, 2466–2470.

Tombes, R. M., Simerly, C., Borisy, G. G. & Schatten, G. (1992). Meiosis, egg activation, and nuclear envelope breakdown are differentially reliant on Ca^{2+}, whereas germinal vesicle breakdown is Ca^{2+} independent in the mouse oocyte. *Journal of Cell Biology* **117**, 799–811.

Whitaker, M. & Patel, R. (1990). Calcium and cell cycle control. *Development* **108**, 525–542.

Acknowledgements

The authors thank Drs Y. Kawakami, S. Mitani, and S. Oda for discussions and suggestions, Dr Y. Nakano and Mr T. Ohira for their technical assistance, and also Dr Laurinda A. Jaffe for valuable comments on the manuscript. This work was supported by a Grant-in-Aid for General Scientific Research from the Japan Ministry of Education, Science, Sports, and Culture.

Received 5 December 1995; accepted 15 February 1996.